Bakker A., Fasano J.B., Myers K.J. (1994) Effects of Flow Pattern on the Solids Distribution in a Stirred Tank. 8th European Conference on Mixing, September 21-23, 1994, Cambridge, U.K. IChemE Symposium Series No. 136, ISBN 0 85295 329 1, page 1-8.

EFFECTS OF FLOW PATTERN ON THE SOLIDS DISTRIBUTION IN A STIRRED TANK

André Bakker and Julian B. Fasano
Chemineer, Inc.
5870 Poe Avenue, Dayton, OH 45401-1123, USA

Kevin J. Myers
Department of Chemical and Materials Engineering
University of Dayton, Dayton, OH 45469-0246, USA

The relation between the flow pattern and the spatial distribution of the solids in a stirred tank has been investigated. Both single impeller systems and multiple impeller systems were studied in tanks with a liquid level of up to 1.75 times the tank diameter, using pitched blade turbines and high efficiency impellers. A variety of techniques was used including visual observation, streakline photography and mathematical modeling.

The solids distribution is strongly affected by certain flow transitions. When the impeller diameter and/or impeller-bottom clearance are too large, the flow direction at the bottom reverses, seriously hampering solids suspension.

Adding a second impeller does not decrease the just-suspended speed. A second impeller does increase the homogeneity of the suspension, provided that the spacing between the impellers is not too large.

1. INTRODUCTION

Traditionally stirred tanks for solids suspension applications have been designed using the just-suspended impeller rotational speed N_{js}, as defined by Zwietering [1]. Although much work about solids suspension has been published, most of it concentrated on correlating N_{js} in a form similar to Equation (1):

$$N_{js} = s X^a D^{-b} d_p^c \left(\frac{\rho_s - \rho_l}{\rho_l}\right)^d \left(\frac{D}{T}\right)^e \left(\frac{C}{T}\right)^f u_t^g \qquad (1)$$

The proportionality constant s is assumed to be a function of impeller type only. Attempts to develop mathematical models for the solids suspension process are often based on the total power draw of the impeller or the average liquid velocity in the tank, without taking local effects into account.

The effect of the flow pattern on the spatial distribution of the solids has received relatively little attention. This relation is the topic of this paper. A variety of techniques is used including visual observation, streakline photography, and mathematical modeling. Both single impeller systems and multiple impeller systems are studied, using pitched blade turbines and high efficiency axial flow impellers.

2. EXPERIMENTAL

Flow patterns were studied experimentally using streakline photography. The tank is illuminated with a light sheet, approximately 0.02 m thick. Neutrally buoyant, translucent particles are added to the tank. When photographs are taken with an appropriate shutter speed, particles that move through the light sheet show up as streaks.

The tank used in these flow visualization studies had a diameter of T = 0.29 m. The liquid level was Z = 0.51 m. Several impeller types, sizes and combinations were studied.

Several tanks, ranging in size from 0.15 m diameter to 1.5 m diameter were used in the solids suspension studies. N_{js}, fillet volume and cloud height were all determined visually. Various solids were studied, with terminal settling velocities ranging from 1.3E-03 m/s to 0.33 m/s).

3. MODELLING

Fluent™ was used to calculate the single phase flow patterns. Experimental velocity data, obtained through laser Doppler velocimetry (LDV), were used as boundary conditions for the impellers.

The single-phase flow pattern is then used as input for GHOST! (Gas Holdup Simulation Tool!). This code was originally developed to study gas-liquid flows but has been extended to solid-liquid mixtures. GHOST! calculates the spatial distribution of the solids from the continuity equation and the momentum balance for the solids. The continuity equation is modelled as:

$$\vec{\nabla}.(\alpha\,\vec{u}_s) + \vec{\nabla}.(\vec{\nabla}(D_s\alpha)) = 0 \qquad (2)$$

Here α denotes the local volume fraction of solids; $\vec{u}_s$ denotes the linear velocity of the solids and D_s is the turbulent diffusion coefficient for the solids. The first term on the left describes the convective transport of solids that results from the mean flow, while the second term describes the turbulent transport of the solids. The turbulent diffusion coefficient for the solids is modeled by an analogy with the kinetic gas theory, see Bakker [2]:

$$D_s = \frac{\sqrt{k}}{3\,\pi\, n_p\, d_p^2} \qquad (3)$$

Here n_p is the particle number density, d_p is the particle diameter and k is the turbulent kinetic energy density in the liquid phase. Instead of calculating the time-averaged linear velocity of the solids from the momentum balance of the solids it was assumed that the solids had a constant slip velocity relative to the liquid phase in the axial direction, equal to the terminal settling velocity:

$$\vec{u}_s = \vec{u}_l + \vec{u}_t \qquad (4)$$

GHOST! calculates the local solids volume fraction α from equations (2)-(4). Particle-particle interactions and the effects of the solid particles on the average liquid flow are not taken into account. A more extensive discussion and justification of the model is given by Bakker [2] and Bakker and Van den Akker [3].

4. RESULTS FOR SINGLE IMPELLER SYSTEMS

Two axial flow impellers were studied, a pitched blade turbine (P-4) and a high efficiency impeller (Chemineer HE-3), see Fig. 1. For both impellers the just-suspended speed, the cloud height and the fillet volume were measured for a variety of solids and various D/T and C/T ratios.

Provided that the C/T and/or D/T ratios are not too large, both types of impeller will generate an axial jet that sweeps the tank bottom of settled solids. This type of flow pattern is depicted in Figure 2. The flow at the bottom is mainly directed outward. The Fluent particle tracking model was used to study the movement of particles through the tank for this situation, see Figure 3. The particles move throughout the whole tank, only temporarily settling in slow moving regions in the center of the tank and behind the baffles. Particles that settle behind the baffles are swept up by the vortex motion in this region, which is also visible in Figure 3.

When the clearance and/or the impeller diameter are increased, a flow transition occurs, as shown in Figure 4. The outflow of the impeller is now more radial and the jet from the impeller is directed towards the vessel wall. The flow direction at the tank bottom is reversed and is now directed inward, rather than outward as was the case with the axial flow pattern. Such a reversed flow at the vessel base was also found by Jaworski *et al.* [4], using laser Doppler Velocimetry. Also the velocities at the bottom are lower than with the axial flow pattern. As a result, complete solids suspension is much more difficult to obtain with this flow pattern. Figure 5 shows that now the solids mainly move around at the tank bottom, instead of being suspended throughout the vessel.

This flow reversal causes an impractical increase in N_{js}, that can not easily be correlated with an equation of the form of Equation (1). For most solids suspension applications the impellers should therefore be operated in the axial flow regime. Figure 6 shows the flow regime of the impeller as a function of C/T and D/T. Notice that the HE-3 impeller can be used at larger values of C/T and D/T than the P-4, thus providing greater flexibility when designing a solid-liquid system.

Figure 7 shows the power draw at just-suspended conditions as a function of D/T ratio. Both the P-4 and the HE-3 have a minimum around D/T = 0.35. The just-suspended power draw increases at very small and very large D/T ratios. At small D/T ratios the velocities at the vessel base near the tank wall are too small to suspend the solids. When the D/T ratio is very large the outflow of the impeller becomes more radial and solids settle at

the center of the vessel base. As a result, models that are only based on overall power draw of the impeller system will not be able to accurately predict the just-suspended speed and power draw.

Figure 8 (from [5]) shows the cloud height as measured visually at N_{js} as a function of D/T ratio. At just-suspended conditions, the cloud height increases with increasing D/T ratio. This shows that although N_{js} gives information about the events on the tank bottom, N_{js} is not directly related to the uniformity of the suspension.

5. MULTIPLE IMPELLER SYSTEMS

The effect of adding a second impeller on N_{js} was studied. Figure 9 (from [5]) shows that the effect of the second impeller is small and generally less than 5%. However, the second impeller can increase the uniformity of the suspension. Mak and Ruszkowki [6] obtained similar results for pitched blade turbines.

Figures 10a, 10b and 10c show the flow pattern in a tank with one HE-3 impeller, two HE-3 impellers with a spacing of S = 3 D and a tank with two HE-3 impellers with a spacing of S = 3.7 D. All three impeller systems have the same D/T ratio and draw the same power. The multiple impeller systems were operated at $N_{js} = 7.6\ s^{-1}$ and the single impeller system was operated at $1.27\ N_{js} = 9.6\ s^{-1}$. Figure 10 shows that the single impeller generates one flow loop, extending to about half the liquid level. The two impellers spaced at S/D = 3 generate one large flow loop. When the impeller spacing is increased to S/D = 3.7, the flow between the impellers separates and two flow loops are formed.

The flow pattern has a profound effect on the solids distribution in the tank. With the single impeller the solids do not move up higher than about half the liquid level, as shown in Figure 11a. When a second impeller is added such that one long flow loop is formed the solids reach the level of the second impeller, as shown in Figure 12b. When the second impeller is placed too far above the first impeller and zoning occurs, the solids do not reach the upper impeller. From the differences between the solids suspension performance of the three impeller systems it can be concluded that designing based on only N_{js} or on power draw does not necessarily lead to an optimum design. The impeller system has to be designed such that it provides the optimum flow pattern for the suspension duty to be performed.

The modelling results shown in Figures 10 and 11 were experimentally verified. Figure 12 shows streakline photographs for the impeller geometries from Figure 10. These photographs show flow patterns similar to the results of the mathematical simulation. However, since the flow is turbulent the streakline photographs show more chaotic flows than the time averaged computer simulations. Figure 13 shows the experimentally found cloud heights for these systems. Also these photographs confirm the conclusions drawn from the modelling results presented in Figure 11.

6. CONCLUSIONS

The solids spatial distribution is strongly affected by certain flow transitions. When the impeller diameter to tank diameter ratio (D/T) and/or impeller off bottom clearance are too large, a flow transition with reversed flow directions at the vessel base may occur. This results in an impractical increase in the just suspended impeller speed N_{js}.

With respect to power draw, the optimum D/T ratio to achieve just-suspended conditions is around D/T = 0.35 for both the P-4 and the HE-3.

Adding a second impeller has a very small effect on the just suspended speed. In multiple impeller systems zoning occurs when the impeller separation distance is too large. It is found that the most efficient solids mixing occurs just before the flow between the impeller separates.

Designing on the basis of N_{js} or on the basis of power consumption does not necessarily lead to an optimum impeller system. To design an optimum impeller system the effects of the flow pattern on the solids distribution must be taken into account. Computer simulation provides an excellent tool to quickly study the effect of impeller system on solids distribution.

REFERENCES

[1] Zwietering, Th. N., 1958, Chem. Eng. Sci., 8, Page 244-253

[2] Bakker, A., 1992, Ph.D. Thesis, Delft University of Technology, The Netherlands

[3] Bakker, A., Van den Akker, H.E.A., 1991, Proc. 7th Eur. Conf. on Mixing, page 199-208, Brugge, Belgium

[4] Jaworski, Z., Nienow, A.W., Koutsakos, E., Dyster, K., Bujalski, W., 1991, Trans. I. Chem. E., Vol. 69, Part A, July 1991, Page 313-320

[5] Hicks, M.T., 1993, M.Sc. Thesis, Dept. of Chemical & Materials Engineering, University of Dayton, Dayton OH, USA

[6] Mak, A., Ruszkowski, S.W., 1991, FMP Interim Report 1063, BHR Group Ltd.

SYMBOLS

C	Impeller off-bottom clearance	(m)
d_p	Particle diameter	(m)
D_s	Turbulent diffusion coefficient for the solids	($m^2.s^{-1}$)
k	Turbulent kinetic energy density	($m^2.s^{-2}$)
H_c	Cloud height	(m)
n_p	Particle number density	(m^{-3})
N_{js}	Impeller rotational speed at just-suspended conditions	(s^{-1})
s	Impeller dependent proportionality constant in N_{js} correlation	(-)
S	Impeller separation distance in multiple impeller systems	(m)
u_l	Liquid linear velocity	($m.s^{-1}$)
u_s	Solids linear velocity	($m.s^{-1}$)
u_t	Particle terminal settling velocity	($m.s^{-1}$)
Z	Liquid level	(m)
α	Volume fraction of solids	(-)
ρ_l	Liquid density	($kg.m^{-3}$)
ρ_s	Solids density	($kg.m^{-3}$)

TRADEMARKS

Fluent™ is a trademark of Fluent Inc., Lebanon, NH 03766, USA

ACKNOWLEDGEMENT

The authors gratefully acknowledge the contribution of Michael T. Hicks.

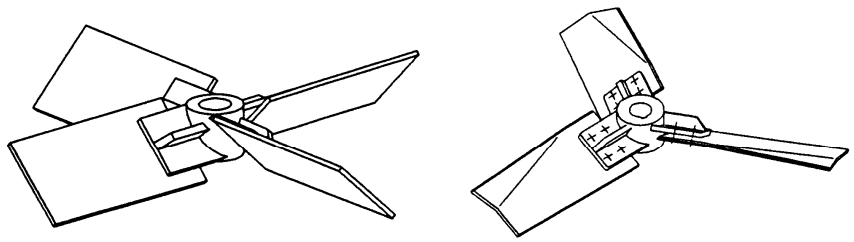

Figure 1 - Four blade pitched blade turbine (P-4) and three blade high efficiency impeller (Chemineer HE-3)

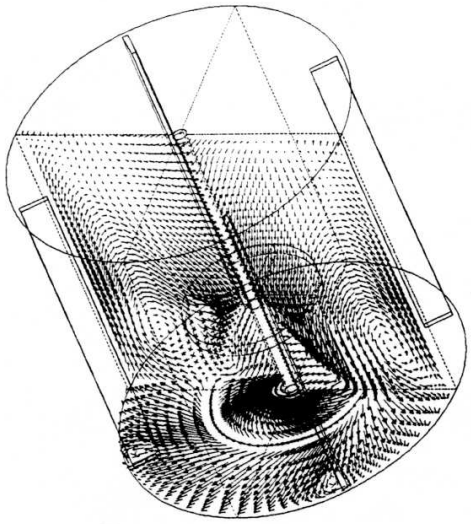

Figure 2 Axial flow pattern with a P-4 impeller. D/T = 0.4; C/T = 0.33;

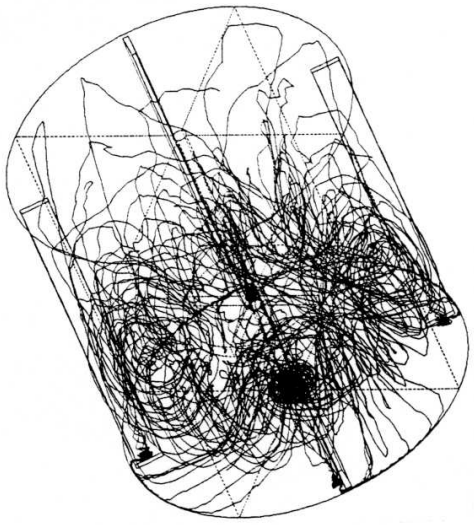

Figure 3 Trajectories of solid particles in the tank of Figure 2.

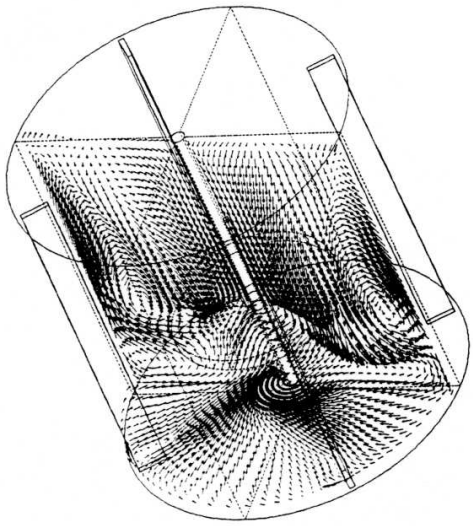

Figure 4 Reversed flow direction near the vessel bottom with a D/T = 0.5 P-4 impeller operated at the same torque as the D/T = 0.4 impeller in Figure 3.

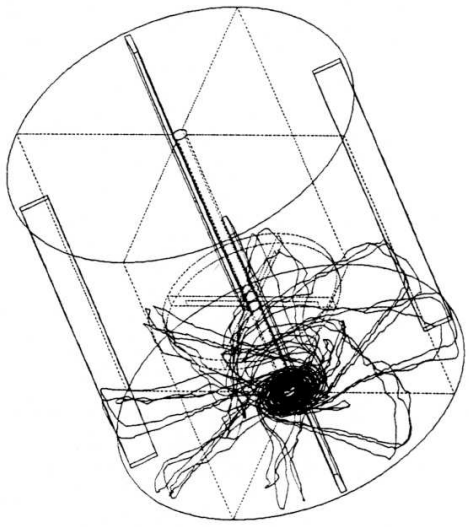

Figure 5 Trajectories of solid particles in the tank of Figure 4.

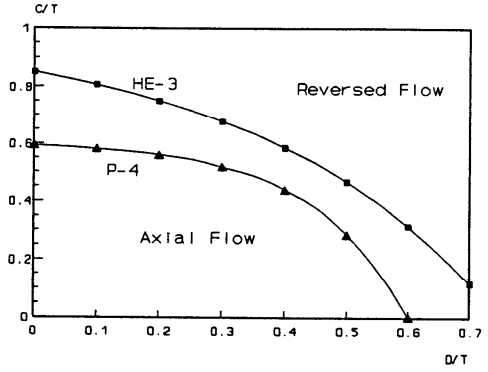

Figure 6 Flow regime as a function of C/T and D/T.

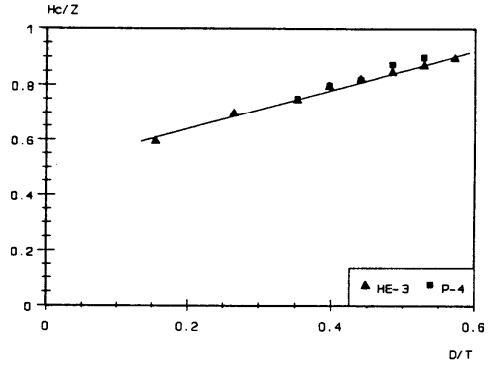

Figure 8 Cloud height H_c at N_{js} vs. D/T.

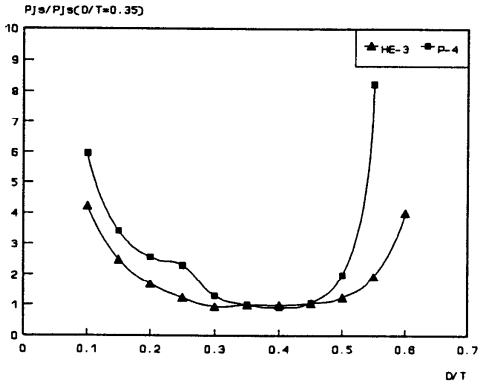

Figure 7 Power draw at just-suspended conditions vs. D/T. Power draw normalized with P_{js} at D/T = 0.35.

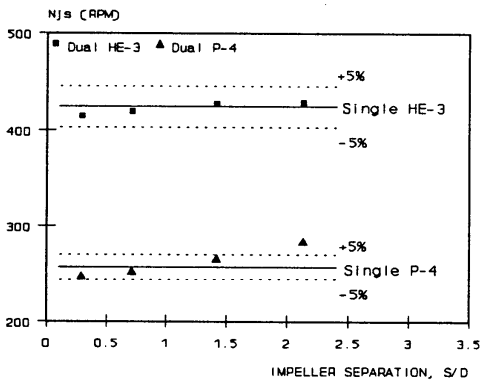

Figure 9 Datapoints show N_{js}(RPM) for dual impeller systems vs. impeller separation distance. Lines are for single impeller systems. T=0.29 m; D/T=0.35; C_1/T=0.25; X=3.33%; U_t=0.077 m/s.

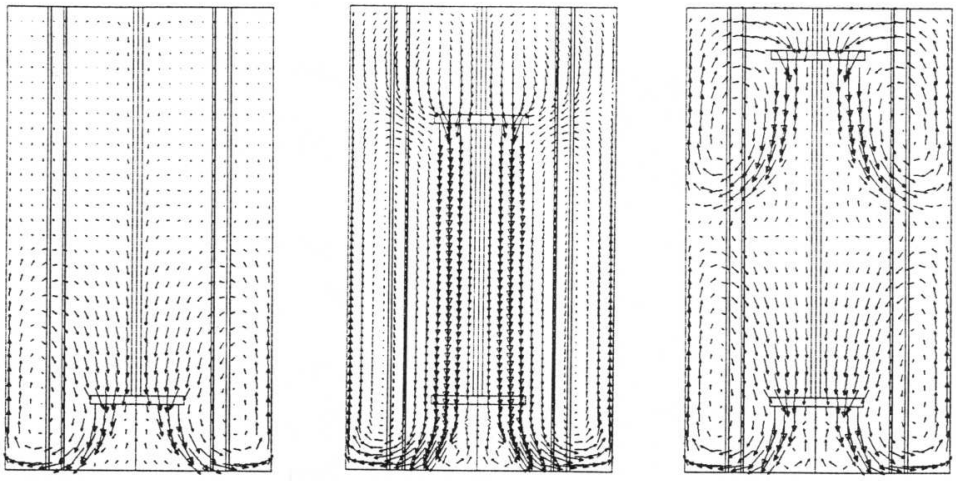

Figure 10a,b,c Simulated flow patterns for a single HE-3, a double HE-3 with a spacing of S/D = 3 and a double HE-3 with a spacing of S/D = 3.7.

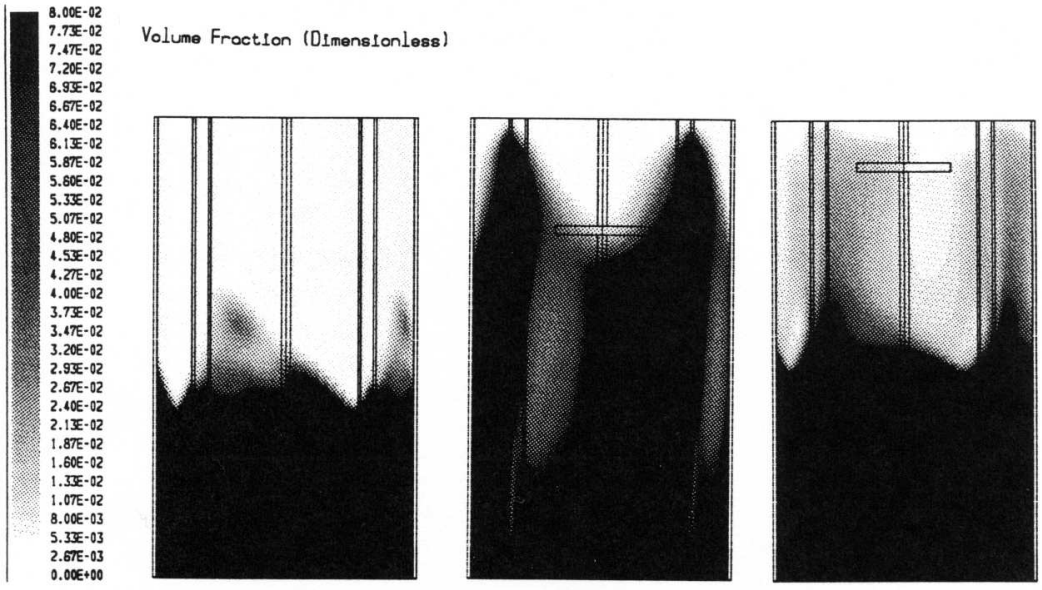

Figure 11a,b,c Simulated solids concentrations at the tank wall(!) for the impeller systems of Figure 10a,b,c. Dark is a high solids concentration and light is a low solids concentration.

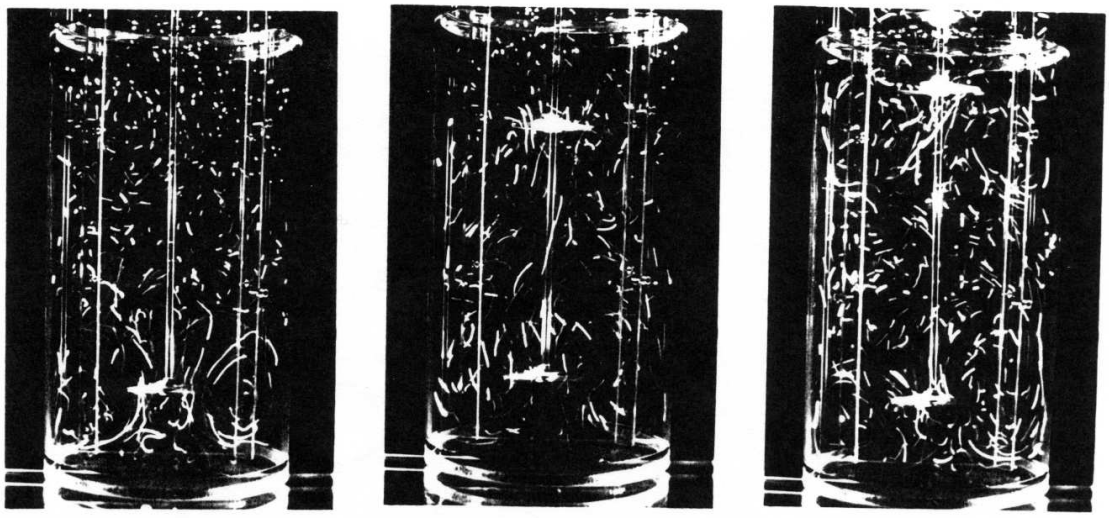

Figure 12a,b,c Streakline photographs for the impeller systems of Figure 10 and 11. The length of the streaks is proportional to the liquid velocity.

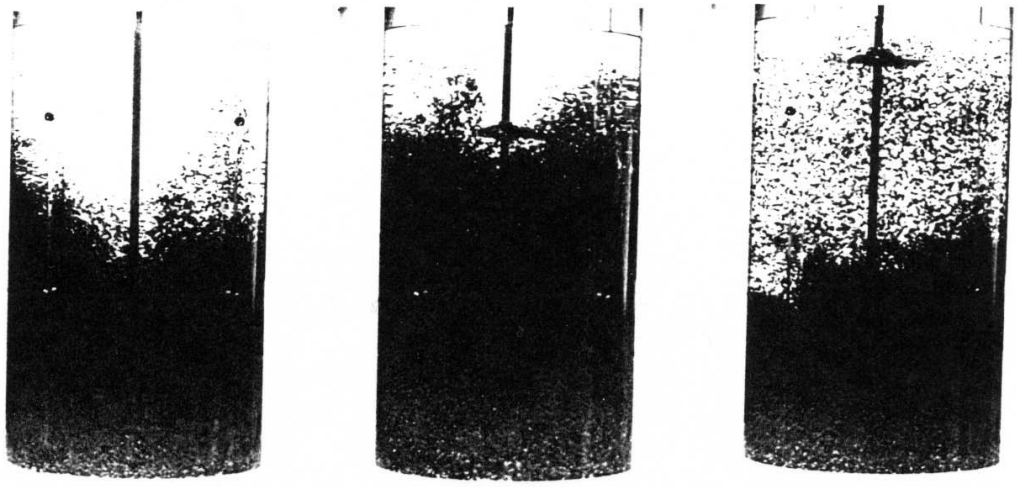

Figure 13a,b,c Experimental solids concentration at the tank wall for the impeller systems of Figures 10, 11 and 12.